



HHS Public Access

Author manuscript

IEEE Trans Ultrason Ferroelectr Freq Control. Author manuscript; available in PMC 2022 January 01.

Published in final edited form as:

IEEE Trans Ultrason Ferroelectr Freq Control. 2021 January ; 68(1): 21–28. doi:10.1109/TUFFC.2020.3005670.

Transcranial Focused Ultrasound for Non-invasive Neuromodulation of the Visual Cortex

Gengxi Lu,

Roski Eye Institute, Keck School of Medicine, University of Southern California, Los Angeles, CA 90033, USA

Department of Biomedical Engineering and NIH Resource Center for Medical Ultrasonic Transducer Technology, University of Southern California, Los Angeles, CA 90089, USA

Xuejun Qian,

Roski Eye Institute, Keck School of Medicine, University of Southern California, Los Angeles, CA 90033, USA

Department of Biomedical Engineering and NIH Resource Center for Medical Ultrasonic Transducer Technology, University of Southern California, Los Angeles, CA 90089, USA

Johnny Castillo,

Roski Eye Institute, Keck School of Medicine, University of Southern California, Los Angeles, CA 90033, USA

Runze Li,

Roski Eye Institute, Keck School of Medicine, University of Southern California, Los Angeles, CA 90033, USA

Department of Biomedical Engineering and NIH Resource Center for Medical Ultrasonic Transducer Technology, University of Southern California, Los Angeles, CA 90089, USA

Laiming Jiang,

Roski Eye Institute, Keck School of Medicine, University of Southern California, Los Angeles, CA 90033, USA

Department of Biomedical Engineering and NIH Resource Center for Medical Ultrasonic Transducer Technology, University of Southern California, Los Angeles, CA 90089, USA

Haotian Lu,

Department of Biomedical Engineering and NIH Resource Center for Medical Ultrasonic Transducer Technology, University of Southern California, Los Angeles, CA 90089, USA

K. Kirk Shung [Fellow, IEEE],

Department of Biomedical Engineering and NIH Resource Center for Medical Ultrasonic Transducer Technology, University of Southern California, Los Angeles, CA 90089, USA

Mark S. Humayun [Fellow, IEEE],

Roski Eye Institute, Department of Ophthalmology, University of Southern California, Los Angeles, CA 90033, USA

Department of Biomedical Engineering, University of Southern California, Los Angeles, CA 90089, USA

Biju B. Thomas,

Roski Eye Institute, Keck School of Medicine, University of Southern California, Los Angeles, CA 90033, USA

Qifa Zhou [Fellow, IEEE]

Roski Eye Institute, Department of Ophthalmology, University of Southern California, Los Angeles, CA 90033, USA

Department of Biomedical Engineering, University of Southern California, Los Angeles, CA 90089, USA

Abstract

Currently, blindness cannot be cured and patients' living quality can be compromised severely. Ultrasonic neuromodulation is a promising technology for the development of non-invasive cortical visual prosthesis. We investigated the feasibility of transcranial focused ultrasound (tFUS) for non-invasive stimulation of the visual cortex to develop improved visual prosthesis. tFUS was used to successfully evoke neural activities in the visual cortex (VC) of both normal and retinal degenerate (RD) blind rats. Our results showed that blind rats showed more robust responses to ultrasound stimulation compared to normal rats. ($p < 0.001$, two-sample *t*-test). Three different types of ultrasound waveforms were used in the three experimental groups. Different types of cortical activities were observed when different US waveforms were used. In all rats, when stimulated with continuous ultrasound waves, only short-duration responses were observed at 'US on & off' time points. In comparison, pulsed waves evoked longer low-frequency responses. Testing different parameters of pulsed waves showed that a pulse repetition frequency higher than 100Hz is required to obtain the low-frequency responses. Based on the observed cortical activities, we inferred that acoustic radiation force (ARF) is the predominant physical mechanism of ultrasound neuromodulation.

Keywords

cortical visual prosthesis; genetically blind rats; transcranial focused ultrasound; ultrasound stimulation; visual cortex

I. Introduction

Recent studies have shown that tFUS is a promising non-invasive technology for cortical neuromodulation. Ultrasound waves pass through the skull and stimulate almost any area of the brain with precise spatiotemporal resolution. Meanwhile, the safety of tFUS has been proved in many *in-vivo* studies in various animal models [1–8] and humans [9–13]. While electrical stimulation methods offer high targeting specificity and resolution, invasive cranial surgery is required. Further, electrode implantation and its maintenance cause problems,

especially for long-term deep brain stimulation [14, 15]. Other non-invasive brain stimulation methods such as temporally interfering electric fields [16], repetitive transcranial magnetic stimulation (TMS) and transcranial direct current stimulation (tDCS) [17, 18] have relatively poor spatial resolution (on the order of centimeters) compared to tFUS (on the order of few millimeters). Additionally, it is difficult for TMS and tDCS to modulate deep subcortical areas.

Age-related macular degeneration (AMD) and retinitis pigmentosa (RP) are two common outer retinal degenerative (RD) diseases that can produce severe vision loss. It is estimated that nearly 30% of the U.S. population greater than 75 years of age have AMD, 10% of whom may become legally blind [19–21]. Currently there is no cure for blindness resulting from end-stage AMD and RP. Retinal prosthesis use electrical stimulation to directly elicit neural activity at the inner retina and promise the best short-term strategy to provide partial restoration of sight to the blind [20, 22–24]. In retinal prosthesis, electrically induced neural activities are transmitted through the optic nerve to the higher visual areas of the brain to obtain visual perception. There are also visual prosthetic devices based on directly stimulating the visual cortex, such as the Orion System by Second Sights Inc. This cortical visual prosthesis converts images captured by a miniature video camera mounted on a patient's glasses into electrical pulses transmitted wirelessly to an array of electrodes on the surface of the visual cortex. Although several types of visual prosthesis have been developed, they all are reported to have severe limitations (references). Firstly, current technologies have limited spatial resolution due to the limited number of stimulating electrodes. Secondly, invasive devices require complex and difficult surgical implantation procedures. They also cause significant issues including encapsulation, electrode degradation, and interference with residual vision resulting from limitations in biocompatibility and power supply. Blindness can also occur due to irreversible and permanent inner retinal damages caused by glaucoma, optic neuropathy diseases, or accidents. Treating the above conditions by stimulating the retina may not be very effective. Direct implantation of the prosthesis into the visual cortex (VC) is an alternate option that has the advantage of avoiding device implantation in the delicate retinal tissue. However, the majority of the issues associated with eye implantation could persist when implanting prosthesis in the brain. In addition, electrical stimulation in the brain may produce side effects because of the strong current used in prosthesis. Therefore, there is an unmet clinical need for developing new techniques to cure blindness.

Non-invasive ultrasonic (US) visual prosthesis has great potential for restoring lost vision and is a promising treatment for patients suffering from blindness. Some studies have shown that tFUS can modulate the neuronal activities of the VC. Seung-Schik Yoo's group used 5% duty cycle tFUS to suppress visually evoked potentials (VEPs) in rats and elevated the VEPs using higher duty cycle and stronger ultrasound intensity [25]. Human studies conducted by the above group suggested that tFUS can stimulate the human VC, resulting in the perception of phosphene and associated evoked potentials. The study also showed a network of activated brain regions that are typically involved in visual and higher-order cognitive processes [10]. In all the above studies, only normal animals and humans without any visual disability were tested. So far, no studies have been conducted to restore vision using tFUS by targeting the VC. In addition to this, the mechanism behind ultrasound neuromodulation

is still undetermined, making it difficult to optimize ultrasonic parameters in various applications.

In this study, we use tFUS to stimulate the VC of normal rats and RD rats with severe retinal degeneration that are considered to be blind. VC-evoked potentials were measured to provide an electrophysiological assessment of the brain activities. Different ultrasonic waveforms were tested, and different types of responses were analyzed. Light-evoked potentials were also measured for comparison with tFUS evoked activities. Our results suggested that tFUS stimulation of the VC in rats can evoke neuronal activities in both normal and RD blind rats. Also, the blind rats showed significantly stronger responses to ultrasound stimulation compared to the normal rats. The results also support the idea that the predominant physical mechanism of ultrasound neuromodulation is the acoustic radiation force (ARF).

II. Materials and Method

A. Ultrasound transducer and waveform

A self-designed 0.5 MHz transducer was used to stimulate the VC, with a center frequency of 0.5 MHz, 23 mm focal length, a f -number of 0.7 for a minimized focal area. A 3D-printed collimated cone was attached to the surface of the transducer for better collimation and easier manipulation in experiments. The transducer was manipulated by a 5-axis stage to aim at VC. A function generator (AFG3252C, Tektronix, Beaverton, OR, USA) was connected to a radiofrequency power amplifier (100A250A, Amplifier Research, Souderton, PA, USA) to drive the transducer. The diagram of experimental system is shown in Fig. 1. Different types of waveforms were used in the three experiment groups:

1. A 15-ms-long continuous wave (CW) following a rest of 6 seconds.
2. Two 2-ms-long continuous waves following a rest of 6 seconds. The interval between two waves was 20 ms.
3. Pulsed waves (PW) with high pulse repetition rate (PRF) were used in group 3. Five sets of parameters were used: 500 Hz PRF with 1-ms pulse, 500 Hz with 0.5-ms pulse, 333.3 Hz PRF with 1-ms pulse, 200 Hz PRF with 2-ms pulse, 100 Hz PRF with 5-ms pulse. All stimulations were conducted for 30 ms following a rest of 6 seconds.

Ultrasound field was measured by the hydrophone (HGL-0400, ONDA, Sunnyvale, CA, USA) in a large water tank (free field). The ultrasonic spatial peak pulse average intensity I_{SPPA} used in all experiments were the same. The spatial-peak temporal-average intensity (I_{SPTA}) was defined as $I_{SPTA} = I_{SPPA} * DC$. DC is the duty cycle (%) of the pulsed waveforms, which were different in three groups.

To better illustrate the acoustic field and the ultrasound-induced temperature increase, a finite-element simulation was conducted using a finite element analysis software. (COMSOL 5.3a, COMSOL Inc., Burlington, MA, USA.)

B. Animal preparation

All animal procedures were approved by the University of Southern California Institutional Animal Care and Use Committee (IACUC). Seventeen rats were studied. Six of them were normally sighted Long-Evan (LE) rats, and eleven were RD Royal College of Surgeon (RCS) blind rats. Three normal rats and three blind rats were used in experimental groups 1&2. Five blind rats were used in group 3. The RCS rats are characterized by retinal pigment epithelium (RPE) dysfunction due to the deletion of the Mer tyrosine kinase (MerTK) receptor that abolishes internalization of photoreceptor (PR) outer segments by RPE cells. All rats were male and about six-month old. The rats were anaesthetized initially with an intraperitoneal injection of Ketamine/Xylazine (50–90 mg/kg, 5–10mg/kg) then with sevoflurane inhalation through a nose cone. [26] The eyes were dilated using 1% tropicamide and 2.5% phenylephrine drops. The cranium was exposed by removing the skin above skull. A small cranial hole was made using a dental drill. All procedures and experiments were performed in a dark room illuminated with dim red light to minimize possible stimulation of the VC due to photoreceptor activation. The space between the brain surface and transducer was filled using US gel.

C. Recording of VC evoked potential activities

A tungsten needle electrode (E363T, P1 Technologies, Roanoke, VA, USA) was advanced into the visual cortex using the stereotactic apparatus. The electrode was aligned to the ultrasound focal area as accurate as possible, as shown in Fig. 1(b). The reference electrode was attached to the scalp and the ground electrode was placed on the hindlimb. Signals were recorded by a PowerLab data acquisition (DAQ) system (ADInstruments, Sydney, Australia). Sampling frequency was 100 kHz. DAQ was synchronized with the ultrasound stimulation and light stimulation. To record light stimulation activities in the brain, a full-field strobe flash using a Grass Photoc stimulator (Grass Instrument Co., W. Warwick, RI, USA) was delivered to the contralateral eye with a 6 second interstimulus interval. The optical stimulation has a duration shorter than <1 ms. In all experiments, recordings were repeated eight times. For each recording, the signals were averaged 64 times. Two filters together with 60Hz notch filter were applied to all signals. The 300 Hz-25000 Hz filter highlights the short-time/high-frequency responses which were clearly observed in only groups 1&2 (CW ultrasound). In contrast, the 0.1 Hz-300 Hz filter highlights the long-time/low-frequency responses which were observed only in group 3 (PW ultrasound). Light stimulation signals were filtered with a 60 Hz notch filter. The amplitude of the evoked potentials was used to quantify the stimulation effects in this study. Signal processing and statistical analysis were conducted using MATLAB 2017a (Mathworks, Natick, MA, USA).

D. Experimental design

The major difference between the three experimental groups was that different ultrasound waveforms were used. All animals went through the same experimental procedures: baseline recording, light stimulation, ultrasound stimulation and no stimulation control recording. There were 5 minutes intervals between each step. During the control recording, the ultrasound was still on, but the transducer was oriented to a completely different location (away from the brain).

III. Results

A. Ultrasound field

The measured focused ultrasound pressure in free field had a peak-to-peak amplitude of 3.74 MPa, the intensity I_{SPPA} was 115.8 W/cm^2 , the mechanical index (MI) was 2.6. The -6dB focal area had a lateral width of 2.4 mm, and an axial length of 5.1 mm. A stimulated ultrasound field has been shown in Fig. 1(c). Ultrasound heating effect can be neglected giving the relatively low center frequency, and short stimulation time (in the order of milliseconds). In the simulation, the absorption coefficient was set to 5 Np/m , which is high for 0.5MHz ultrasound. [27] The stimulation time was set to 100ms which is much longer than the stimulation time in this study ($<15\text{ms}/6\text{s}$). In the bottom of Fig. 1(c), the color represents the increased temperature (K) caused by ultrasound stimulation. With these loose conditions, the increased temperature is lower than 0.3°C .

The center frequency of ultrasound was chosen as 0.5MHz mainly based on two aspects: skull penetration and focal size. Lower frequency provides a better penetration and worse resolution. Considering the surface topography of rat brain as shown in Fig. 1(b), the focus should have a diameter smaller than 4mm for a region specific stimulation of visual cortex [28]. Higher-frequency ultrasound will be strongly distorted by the skull. Therefore, 0.5MHz is chosen as the center frequency in this study, which has also been widely used in various ultrasound neuromodulation studies. For safety concern, amplitude of ultrasound was determined to be as low as possible to see clear responses. Amplitude was same in all experimental groups.

B. VC responses from groups 1&2

Representative results from one LE normal rat and one RCS blind rat are shown in Fig. 2. During US stimulation, 20-ms-long signals were recorded in group 1 rats and 55-ms-long signals were recorded in group 2 rats. Different durations of CW were tried in the study. The durations from 2ms to 15ms caused similar responses, except that both ‘on&off’ responses can be observed in 15-ms-CW stimulation on blind rats and cannot be observed in 2-ms-CW stimulation. Initially, light stimulation was used to test the rats’ visual sense, Figs. 2(a)&(e) for which 20-ms-long signals were recorded. The light stimulation responses from the normal rat had a peak-to-peak amplitude of $\sim 15 \mu\text{V}$, while the blind rats did not show any light-evoked cortical activities. US-evoked cortical responses were obtained from both normal rats and blind rats. The peak-to-peak amplitude of US responses are summarized in Fig. 3. The US responses from blind rats were significantly stronger than those from normal LE rats ($p < 0.001$, two-sample *t*-test). Looking into the response onset latency and response duration, light responses had a latency $\sim 1 \text{ ms}$ and a duration $\sim 2 \text{ ms}$. In both LE and RCS rats, the US-evoked activities showed latencies comparable to the light-responses ($\sim 1 \text{ ms}$). The response duration was considerably longer during US stimulation ($\sim 5 \text{ ms}$).

C. VC responses from groups 3

In group 3, 30-ms-long pulsed waves were used to stimulate the VC. Different sets of parameters (duty cycle, duration and PRF) were tested. Each set of parameters was tested on one blind rat. US responses from different waveforms are shown in Fig. 4. 100-ms-long

signals were recorded and averaged at 512 times. Different duty cycles (DC), PRFs, and pulse lengths were compared. The evoked potentials had a similar specific waveform: starting with a weak ~10-ms negative peak (N1) followed by a strong ~10-ms positive peak (P1), then a weaker negative peak (N2) and ending with a ~20-ms positive peak (P2). This waveform pattern was observed in all cases except when 5-ms pulse in every 10 ms (100 Hz PRF and 50% DC) was used (see Fig. 4e). Although durations of the peaks were similar, the amplitude of the peaks were different when different stimulation parameters were used.

IV. Discussion

Our study demonstrated that tFUS can evoke VC neuronal activities that are comparable to light stimulated responses. Although US evoked VC potentials observed in our study were weaker than light stimulated responses, it is reasonable to predict that the responses would be stronger if a stronger US intensity was used [29]. The results from group 2 demonstrated that ultrasound VC stimulation can produce temporal resolution shorter than 20 ms. Temporal resolution determines the available frame rate and is an important parameter for developing successful visual prosthesis technology. As shown in Fig. 2, regardless of the degree of US response, the durations were always around 5 ms that provides a potential frame rate of 200 frame/s. It should be noted that the responses in group 2 were slightly longer than the responses in group 1, especially in blind rats. Presumably, this is a result of the overlap between the US-evoked 'on' and 'off' responses.

A key point of our work is the finding that US-evoked VC activities in blind RCS rats were different from those of the normal LE rats. Under the same stimulus conditions, the responses in blind rats were significantly stronger than that of normal rats. During US stimulation, both 'on' & 'off' responses were clearly visible in blind rats whereas only a single peak (apparently 'on' response) was recorded from normal rats. One possible explanation for the differences is that stimulation sensitivity of blind rats' VC has been changed due to prolonged visual deprivation. It is highly unlikely that such differences can be attributed to difference in rat strains. Further investigations using the same animal strains can provide a better conclusion in this regard.

Another major finding of this study is that different ultrasound waveforms can evoke different types of VC responses. In experimental group 3, PW was used to stimulate the VC. Besides the ~5 ms duration responses, which can be shown using a high-pass filter, a different type of long-duration low-frequency response was acquired. As shown in Fig. 4, this type of responses had a duration longer than 20ms with four peaks (N1, P1, N2, P2) at specific time points. The above waveform pattern persisted at different stimulus parameters until the PRF went down to 100 Hz (Fig. 4e). Different DCs were tested at 100 Hz PRF, but the typical waveform was never observed. PRF down to 50 Hz were also tested to confirm that the above waveform cannot be observed at lower PRF. Although the data obtained from group 3 was not sufficient to show statistically significant differences based on various parameters tested (pulse length, PRF, DC), it showed a clear trend to support the hypothesis that PRF larger than 100 Hz are essential to obtain the low-frequency responses. In group 1 & 2, 2-ms waves and 15-ms waves were used to show similar short duration responses. Kim Butt Pauly's group used 80-ms-long US stimulation to the auditory cortex to obtain 'US on

& off^{*} short-duration responses that are comparable to our observation [30]. It can be inferred that changes in the duration of CW stimulation (at least within the range of 100 ms) may not cause changes in the response pattern like PW.

In this study, the acoustic field was measured in free field and the MI was 2.6, which is a little higher than U.S. Food and Drug Administration (FDA)'s limitation of ultrasound imaging 1.9. However, since the MI was measured in free field, it is reasonable to predict that the real acoustic energy that reached the brain would be weaker than the reported pressure, due to the distortion caused by skull and tissue absorption. It is estimated that, the ultrasound transmission factor through the adult rats skull is around 0.5–0.7 at 0.5MHz [31, 32], which will reduce the MI from 2.6 to 1.3–1.8. (<1.9). Therefore, considering the distorting caused by skull, the MI in this study should be within the FDA limitation.

There are some limitations in this study that need to be addressed in future investigations. Rats of different sex and age should be compared. Additional sets of stimulus parameters are required for PW stimulation to validate the effect of individual stimulus condition. We are not ruling out the possibility of backward projections along visual pathways. This can be investigated by suitable staining techniques like C-FOS detection to map the activated neurons. It may also help to understand the extent of spatial resolution. We plan to implement these for our future experiments.

There have been arguments about whether the ultrasound neuromodulation effect in the VC may be partially due to the auditory response to the audible sound caused by pulsed ultrasound or mode conversion [33]. The study from Hubert Lim's group suggested that the removal of cochlear fluids (CF) or transection of the auditory nerves would eliminate the US neuromodulation effect [6]. But Kim's research disproved this argument by eliminating peripheral auditory pathway activation and obtaining motor responses during US stimulation [30]. Although genetically deaf rats or CF removal is required in our future studies to completely eliminate the auditory pathway effects, we conducted some preliminary experiments to rule out its contribution to VC activation. We stimulated the auditory cortex but did not observe any responses at VC. One of the potential factors that causes the arguments and inconsistency among different studies is the stimulation area relative to the animal size, which is related to the animal model, ultrasound frequency and ultrasound focusing. Minimized ultrasound focal point and localized stimulation area are desirable to minimize the experimental artifacts.

Physical mechanism of *in-vivo* ultrasound neuromodulation effect is another significant but undetermined question. Understanding the mechanisms of ultrasound neuromodulation can be helpful in optimizing ultrasonic parameters in various applications and scientific research. Recent studies using excised retinas support the idea that acoustic radiation force (ARF) is the main mechanism for ultrasound-evoked neuronal activities [29] *ex vivo*. The above study ruled out the cavitation effect by comparing the stimulation effect induced by different-frequency ultrasounds with same intensity. However, the study did not discuss the acoustic oscillation effect and the mechanism could be different under *in vivo* conditions. Our *in vivo* results suggest that ARF is the predominant mechanism for ultrasound neuromodulation from another perspective. The two phenomena observed in our experiments - the presence of

‘US on & off’ responses and response changes caused by changes in the PW and CW, support the ARF hypothesis. The candidates for physical mechanism of US stimulation are cavitation, acoustic oscillation, thermal effect, and ARF. However, thermal effect is a gradual and accumulative effect depositing energy in brain tissues, with which PW and CW should not cause different phenomenon [34]. Also, CW should have stronger thermal effect than PW, which was not observed in our experiments. Cavitation effect is the interaction between ultrasound waves and bubbles, where bubbles can be generated if the acoustic pressure has sufficiently negative peaks. The size of the bubble oscillates as the localized pressure changes sinusoidally. Transient cavitation happens when the size expansion is at least double, at which point the bubbles collapse violently, causing a destructive event [35]. In stable cavitation, the size change is smaller and the bubbles do not burst, which is hypothesized to produce stable neuromodulation [29]. Similarly, acoustic oscillation is the intrinsic linear mechanical effect of acoustic waves, which cause tissues sinusoidal oscillations with a much weaker amplitude compared to cavitation effect. ARF is a nonlinear acoustic effect which generates a non-oscillating force and causes a unidirectional displacement in biological tissues [36]. All mechanical acoustic effects are hypothesized to affect local neural ion channels, facilitate cellular ion flux and cause electrical activities of neurons [37–40]. The key difference that highlights the ARF is the fact that ARF has a non-oscillating unidirectional effect, while stable cavitation and acoustic oscillation are sinusoidal and periodic effects. If the stable cavitation or acoustic oscillation is the mechanism, the ion influx and outflux should be periodic as well. It is less likely for periodic effects to cause responses only during ‘US on and off’, and no responses in between. If ARF is the mechanism of neuronal stimulation, the occurrence of the above phenomena is more reasonable. Because the US on can push the neuron or ion channels and cause the measurable electrical potentials, the local potentials will regain the balance (absence of response) until the US is off, which can well explain the ‘on’/‘off’ phenomena observed in our study. We caution that the statement about ARF as the principal physical mechanism of neuromodulation is only a result-oriented interference rather than a well-reasoned conclusion from elaborated experiments. However, we believe that results from this study deserve to be considered in further discussions and in future studies on the mechanisms of ultrasound neuromodulation.

Although the size of ultrasound focus in this study is not fine enough for a practical visual prosthesis, ultrasound has the potential to reach a resolution in micrometer-level by increasing center frequency and enhancing transducer’s focusing performance. In addition, MRI-guided/CT-guided ultrasound technology can enhance the focus region and resolution in further studies.

V. Conclusion

The feasibility of tFUS-based cortical visual prosthesis is studied and discussed here. tFUS can be used to evoke neural activities in the VC of normal and blind rats. Different types of VC responses could be evoked by different US stimulus waveforms. ARF is inferred to be the predominant physical mechanism of ultrasound neuromodulation. Based on our study, ultrasonic neuromodulation is a promising technology for the development of non-invasive

cortical visual prosthesis. It can be applied to treat blindness caused by irreversible inner retinal damages (optic neuropathy or accidents) where retinal prosthesis cannot be effective.

Acknowledgments

This work was supported by the National Institutes of Health (NIH) under grant R01EY026091, R01EY028662, R01EY030126 and NIH P30EY029220. Unrestricted departmental grant from research to prevent blindness.

Biography



K. Kirk Shung obtained a B.S. in EE from Cheng Kung University, Taiwan in 1968 and a Ph.D. in EE from University of Washington, Seattle, WA, in 1975. He has been a professor of biomedical engineering at USC since 2002. He was a dean's professor in biomedical engineering at the Viterbi School of Engineering of USC from 2013–2018 and became the Dwight C. and Hildagarde E. Baum Chair of Biomedical Engineering in 2018.

Dr. Shung is a life fellow of IEEE, and a fellow of American Institute of Ultrasound in Medicine. He is a founding fellow of American Institute of Medical and Biological Engineering. He received the IEEE Engineering in Medicine and Biology Society Early Career Award in 1985 and was the coauthor of a paper that received the best paper award for IEEE Transactions on Ultrasonics, Ferroelectrics and Frequency Control (UFFC) in 2000. He was elected an outstanding alumnus of Cheng-Kung University in Taiwan in 2001. He was selected as the distinguished lecturer for the IEEE UFFC society for 2002–2003. He received the Holmes Pioneer Award in Basic Science from American Institute of Ultrasound in Medicine in 2010, the academic career achievement award from the IEEE Engineering in Medicine and Biology Society in 2011, and IEEE Biomedical Engineering Award in 2016. Dr. Shung has published more than 500 papers and book chapters. He has written two textbooks. He is an associate editor of IEEE Transactions on Biomedical Engineering and Medical Physics. Dr. Shung's research interest is in ultrasonic transducers, high frequency ultrasonic imaging and applications in cellular bioengineering.



Haotian Lu received his B.Eng. degree in Bioengineering from Nanjing Forestry University, Nanjing, Jiangsu, China, in 2018, and the M.Sc. degree in biomedical engineering from University of Southern California, Los Angeles, California, in 2020;

Since 2019, he has been a Research Assistant with the Ultrasonic Transducer Research Center. University of Southern California, Los Angeles. His current research interests

include intravascular ultrasound imaging, additive manufacturing (3D printing) technologies of piezo materials and device systems with controlled micro-architectures and encoded properties.



Johnny Castillo received a Bachelor's of Science degree in Cellular and Molecular Biology from Humboldt State University in May, 2015. Under the guidance of Dr. Qifa Zhou at the University of Southern California, he studied the potential of ultrasound to be used as a molecular tool to modulate neuronal processes in the hippocampus in an *in vivo* Alzheimer's disease rat model. He currently carries out RNA extractions from saliva swabs obtained from patients to diagnose COVID-19 at Curative Inc., San Dimas, CA, USA. His research interest includes the use of ultrasound to deliver genetic elements non-invasively *in vivo* for gene therapeutic purposes, and using electrophysiological techniques to study neurons and retinal ganglion cells in the context of schizophrenia, and retinitis pigmentosa, respectively.



Dr. Laiming Jiang is a Postdoctoral Researcher-Research Associate in the Keck School of Medicine at the University of Southern California (USC). He received his Ph.D. degree in Materials Physics and Chemistry from the Department of Materials Science and Engineering, Sichuan University, in 2019. His research work focuses on lead-free piezoelectric materials, ultrasound transducers/array, energy harvesting, multiscale and multi-materials 3d printing, and bio-implantable devices.



MARK S. HUMAYUN, MD, PHD, is the Cornelius J. Pings Chair in Biomedical Sciences, Professor of Ophthalmology, Biomedical Engineering, and Integrative Anatomical Sciences, Director of the USC Ginsburg Institute for Biomedical Therapeutics, and Co-Director of the USC Roski Eye Institute.

Dr. Humayun is an internationally recognized pioneer in vision restoration. He assembled a team of multidisciplinary experts to develop the first FDA approved artificial retina, Argus II, for sight restoration. He has more than 125 issued patents and over 250 peer reviewed publications. He has a google scholar H index of 90.

Dr. Humayun is a member of the U.S. National Academies of Medicine, Engineering, and Inventors. He was named top 1% of ophthalmologists by the U.S. News & World Report. For his extraordinary contributions he was awarded the United States' highest technological achievement, the 2015 National Medal of Technology and Innovation by President Obama. He is an IEEE Fellow and the recipient of the 2018 IEEE Biomedical Engineering Award and the 2020 IEEE Medal for Innovations in Healthcare Technology.



Biju B. Thomas The laboratory of Biju B. Thomas, PhD focuses on developing new treatment strategies for preventing blindness and/or restoring vision based on drug delivery, small molecules, prosthesis and cell replacement therapies.

Dr. Thomas has designed instruments and techniques for visual functional testing in rodents which were successfully implemented in various research projects. Dr. Thomas has extensive expertise on several scientific and technological disciplines relevant to retinal transplantation research, including subretinal implantation surgeries in rodents, electrophysiological testing of visual function in rodents based on ERG, mfERG and brain stem electrophysiology. Electrophysiological mapping of the superior colliculus (SC), is a state-of-the-art technology that can be used to measure very low level retinal activities from the visual centers (SC and visual cortex) of the brain of rats and mice.



Qifa Zhou received his Ph.D. degree from the Department of Electronic Materials and Engineering at Xi'an Jiaotong University, China in 1993. He is currently a professor of Biomedical Engineering and Ophthalmology at the University of Southern California.

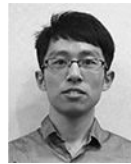
Dr. Zhou is a fellow of the Institute of Electrical and Electronics Engineers (IEEE), the International Society for Optics and Photonics (SPIE), and the American Institute for Medical and Biological Engineering (AIMBE). He is also a member of the Technical Program Committee of the IEEE International Ultrasonics Symposium, and is an Associate Editor of the IEEE Transactions on Ultrasonics, Ferroelectrics, and Frequency Control. His research focuses on the development of piezoelectric high-frequency ultrasonic transducers/array for biomedical ultrasound and photoacoustic imaging, including intravascular imaging, cancer imaging, and ophthalmic imaging. He is also actively exploring ultrasonic mediated therapeutic technology including trans-sclera drug delivery, as well as ultrasound for retinal and brain stimulation. He has published more than 260 peer-reviewed articles in journals including Nature Medicine, Nature Biomedical Engineering, Nature Communication, Science Advanced, Advanced Materials, and IEEE UFFC.



Runze Li received his B.S. degree in Biomedical Engineering from Huazhong University of Science and Technology, Wuhan, China in 2014, and M.S. degree in Biomedical Engineering from University of Southern California, Los Angeles, CA, in 2017. He is currently a Ph.D. student at the Department of Biomedical Engineering of University of Southern California. His research interests include development of high frequency transducer, ultrasonic elastography and optical coherence elastography.



Xuejun Qian received his B.S. degree in electrical engineering from Xidian University, China, in 2012. He received his M.S. degree in electrical engineering and Ph.D degree in Biomedical Engineering from University of Southern California, Los Angeles, CA, USA in 2014 and 2018. He joined NIH Ultrasonic Transducer Resource Center (UTRC) as a Research Assistant under the supervision of Dr. Qifa Zhou and Dr. K. Kirk Shung. His research interests include high-frequency ultrasound elastography, optical coherence elastography, super-resolution microvessel imaging and multi-modality imaging.



Gengxi Lu received his bachelor' degree in Physics from Nanjing University, China, in 2017. He is currently a Ph.D. student at the Department of Biomedical Engineering, University of Southern California, Los Angeles, CA, USA. His research interests include the ultrasound neuromodulation, ultrasound imaging and elastography, development of ultrasound transducers, and photoacoustics.

References

- [1]. Li G, Qiu W, Zhang Z, Jiang Q, Su M, Cai R, Li Y, Cai F, Deng Z, and Xu D, "Noninvasive ultrasonic neuromodulation in freely moving mice," *IEEE Transactions on Biomedical Engineering*, vol. 66, no. 1, pp. 217–224, 2018. [PubMed: 29993389]
- [2]. Zhang Z, Qiu W, Gong H, Li G, Jiang Q, Liang P, Zheng H, and Zhang P, "Low-intensity ultrasound suppresses low-Mg²⁺-induced epileptiform discharges in juvenile mouse hippocampal slices," *Journal of neural engineering*, vol. 16, no. 3, pp. 036006, 2019. [PubMed: 30818304]

- [3]. Li D, Cui Z, Xu S, Xu T, Wu S, Bouakaz A, Wan M, and Zhang S, “Low-intensity focused ultrasound stimulation treatment decreases blood pressure in spontaneously hypertensive rats,” *IEEE Transactions on Biomedical Engineering*, 2020.
- [4]. Legrand M, Galineau L, Novell A, Planchez B, Brizard B, Leman S, Tauber C, Escoffre J-M, Lefèvre A, and Gosset P, “Efficacy of chronic ultrasound neurostimulation on behaviors and distributed brain metabolism in depressive-like mice,” *BioRxiv*, pp. 813006, 2019.
- [5]. Bendau E, Aurup C, Kamimura H, and Konofagou E, “Low intensity, continuous wave focused ultrasound reversibly depresses heart rate in anesthetized mice,” *The Journal of the Acoustical Society of America*, vol. 146, no. 4, pp. 2942–2943, 2019.
- [6]. Guo H, Hamilton M II, Offutt SJ, Gloeckner CD, Li T, Kim Y, Legon W, Alford JK, and Lim HH, “Ultrasound produces extensive brain activation via a cochlear pathway,” *Neuron*, vol. 98, no. 5, pp. 1020–1030. e4, 2018. [PubMed: 29804919]
- [7]. Lee W, Lee SD, Park MY, Foley L, Purcell-Estabrook E, Kim H, Fischer K, Maeng L-S, and Yoo S-S, “Image-guided focused ultrasound-mediated regional brain stimulation in sheep,” *Ultrasound in medicine & biology*, vol. 42, no. 2, pp. 459–470, 2016. [PubMed: 26525652]
- [8]. Verhagen L, Gallea C, Folloni D, Constans C, Jensen DE, Ahnine H, Roumazeilles L, Santin M, Ahmed B, and Lehericy S, “Offline impact of transcranial focused ultrasound on cortical activation in primates,” *Elife*, vol. 8, pp. e40541, 2019. [PubMed: 30747105]
- [9]. Kamimura HA, Lee SA, Niimi Y, Aurup C, Kim MG, and Konofagou EE, “Focused ultrasound stimulation of median nerve modulates somatosensory evoked responses.” pp. 1085–1087.
- [10]. Lee W, Kim H-C, Jung Y, Chung YA, Song I-U, Lee J-H, and Yoo S-S, “Transcranial focused ultrasound stimulation of human primary visual cortex,” *Scientific reports*, vol. 6, no. 1, pp. 1–12, 2016. [PubMed: 28442746]
- [11]. Kubanek J, “Neuromodulation with transcranial focused ultrasound,” *Neurosurgical focus*, vol. 44, no. 2, pp. E14, 2018.
- [12]. Legon W, Sato TF, Opitz A, Mueller J, Barbour A, Williams A, and Tyler WJ, “Transcranial focused ultrasound modulates the activity of primary somatosensory cortex in humans,” *Nature neuroscience*, vol. 17, no. 2, pp. 322, 2014. [PubMed: 24413698]
- [13]. Mueller J, Legon W, Opitz A, Sato TF, and Tyler WJ, “Transcranial focused ultrasound modulates intrinsic and evoked EEG dynamics,” *Brain stimulation*, vol. 7, no. 6, pp. 900–908, 2014. [PubMed: 25265863]
- [14]. Grill WM, “Safety considerations for deep brain stimulation: review and analysis,” *Expert review of medical devices*, vol. 2, no. 4, pp. 409–420, 2005. [PubMed: 16293080]
- [15]. Amon A, and Alesch F, “Systems for deep brain stimulation: review of technical features,” *Journal of Neural Transmission*, vol. 124, no. 9, pp. 1083–1091, 2017. [PubMed: 28707160]
- [16]. Grossman N, Bono D, Dedic N, Kodandaramaiah SB, Rudenko A, Suk H-J, Cassara AM, Neufeld E, Kuster N, and Tsai L-H, “Noninvasive deep brain stimulation via temporally interfering electric fields,” *Cell*, vol. 169, no. 6, pp. 1029–1041. e16, 2017. [PubMed: 28575667]
- [17]. Fregni F, and Pascual-Leone A, “Technology insight: noninvasive brain stimulation in neurology —perspectives on the therapeutic potential of rTMS and tDCS,” *Nature clinical practice Neurology*, vol. 3, no. 7, pp. 383–393, 2007.
- [18]. George MS, and Aston-Jones G, “Noninvasive techniques for probing neurocircuitry and treating illness: vagus nerve stimulation (VNS), transcranial magnetic stimulation (TMS) and transcranial direct current stimulation (tDCS),” *Neuropsychopharmacology*, vol. 35, no. 1, pp. 301–316, 2010. [PubMed: 19693003]
- [19]. Imai H, Honda S, Nakanishi Y, Yamamoto H, Tsukahara Y, and Negi A, “Different transitions of multifocal electroretinogram recordings between patients with age-related macular degeneration and polypoidal choroidal vasculopathy after photodynamic therapy,” *British journal of ophthalmology*, vol. 90, no. 12, pp. 1524–1530, 2006.
- [20]. Weiland JD, Liu W, and Humayun MS, “Retinal prosthesis,” *Annu. Rev. Biomed. Eng.*, vol. 7, pp. 361–401, 2005. [PubMed: 16004575]
- [21]. Curcio CA, Medeiros NE, and Millican CL, “Photoreceptor loss in age-related macular degeneration,” *Investigative ophthalmology & visual science*, vol. 37, no. 7, pp. 1236–1249, 1996. [PubMed: 8641827]

- [22]. Winter JO, Cogan SF, and Rizzo JF, "Retinal prostheses: current challenges and future outlook," *Journal of Biomaterials Science, Polymer Edition*, vol. 18, no. 8, pp. 1031–1055, 2007. [PubMed: 17705997]
- [23]. Dowling J, "Current and future prospects for optoelectronic retinal prostheses," *Eye*, vol. 23, no. 10, pp. 1999–2005, 2009. [PubMed: 19098703]
- [24]. Ryu SB, Werginz P, and Fried SI, "Response of Mouse Visual Cortical Neurons to Electric Stimulation of the Retina," *Frontiers in neuroscience*, vol. 13, 2019.
- [25]. Kim H, Park MY, Lee SD, Lee W, Chiu A, and Yoo S-S, "Suppression of EEG visual-evoked potentials in rats via neuromodulatory focused ultrasound," *Neuroreport*, vol. 26, no. 4, pp. 211, 2015. [PubMed: 25646585]
- [26]. Thomas BB, Aramant RB, Sada SR, and Seiler MJ, "Light response differences in the superior colliculus of albino and pigmented rats," *Neuroscience letters*, vol. 385, no. 2, pp. 143–147, 2005. [PubMed: 15950381]
- [27]. Menikou G, and Damianou C, "Acoustic and thermal characterization of agar based phantoms used for evaluating focused ultrasound exposures," *Journal of therapeutic ultrasound*, vol. 5, no. 1, pp. 14, 2017. [PubMed: 28572977]
- [28]. Gabbott P, and Stewart M, "Distribution of neurons and glia in the visual cortex (area 17) of the adult albino rat: a quantitative description," *Neuroscience*, vol. 21, no. 3, pp. 833–845, 1987. [PubMed: 3627437]
- [29]. Menz MD, Ye P, Firouzi K, Nikoozadeh A, Pauly KB, Khuri-Yakub P, and Baccus SA, "Radiation force as a physical mechanism for ultrasonic neurostimulation of the ex vivo retina," *Journal of Neuroscience*, vol. 39, no. 32, pp. 6251–6264, 2019. [PubMed: 31196935]
- [30]. Mohammadjavadi M, Ye PP, Xia A, Brown J, Popelka G, and Pauly KB, "Elimination of peripheral auditory pathway activation does not affect motor responses from ultrasound neuromodulation," *Brain stimulation*, vol. 12, no. 4, pp. 901–910, 2019. [PubMed: 30880027]
- [31]. O'Reilly MA, Muller A, and Hynynen K, "Ultrasound insertion loss of rat parietal bone appears to be proportional to animal mass at submegahertz frequencies," *Ultrasound in medicine & biology*, vol. 37, no. 11, pp. 1930–1937, 2011. [PubMed: 21925788]
- [32]. Gerstenmayer M, Fellah B, Magnin R, Selingue E, and Larrat B, "Acoustic transmission factor through the rat skull as a function of body mass, frequency and position," *Ultrasound in medicine & biology*, vol. 44, no. 11, pp. 2336–2344, 2018. [PubMed: 30076032]
- [33]. Sato T, Shapiro MG, and Tsao DY, "Ultrasonic neuromodulation causes widespread cortical activation via an indirect auditory mechanism," *Neuron*, vol. 98, no. 5, pp. 1031–1041. e5, 2018. [PubMed: 29804920]
- [34]. Hynynen K, Vykhodtseva NI, Chung AH, Sorrentino V, Colucci V, and Jolesz FA, "Thermal effects of focused ultrasound on the brain: determination with MR imaging," *Radiology*, vol. 204, no. 1, pp. 247–253, 1997. [PubMed: 9205255]
- [35]. Neppiras EA, "Acoustic cavitation," *Physics reports*, vol. 61, no. 3, pp. 159–251, 1980.
- [36]. Rudenko O, Sarvazyan A, and Emelianov SY, "Acoustic radiation force and streaming induced by focused nonlinear ultrasound in a dissipative medium," *The Journal of the Acoustical Society of America*, vol. 99, no. 5, pp. 2791–2798, 1996.
- [37]. Tyler WJ, Lani SW, and Hwang GM, "Ultrasonic modulation of neural circuit activity," *Current opinion in neurobiology*, vol. 50, pp. 222–231, 2018. [PubMed: 29674264]
- [38]. Plaksin M, Shoham S, and Kimmel E, "Intramembrane cavitation as a predictive bio-piezoelectric mechanism for ultrasonic brain stimulation," *Physical review X*, vol. 4, no. 1, pp. 011004, 2014.
- [39]. Krasovitski B, Frenkel V, Shoham S, and Kimmel E, "Intramembrane cavitation as a unifying mechanism for ultrasound-induced bioeffects," *Proceedings of the National Academy of Sciences*, vol. 108, no. 8, pp. 3258–3263, 2011.
- [40]. Fomenko A, Neudorfer C, Dallapiazza RF, Kalia SK, and Lozano AM, "Low-intensity ultrasound neuromodulation: an overview of mechanisms and emerging human applications," *Brain stimulation*, vol. 11, no. 6, pp. 1209–1217, 2018. [PubMed: 30166265]

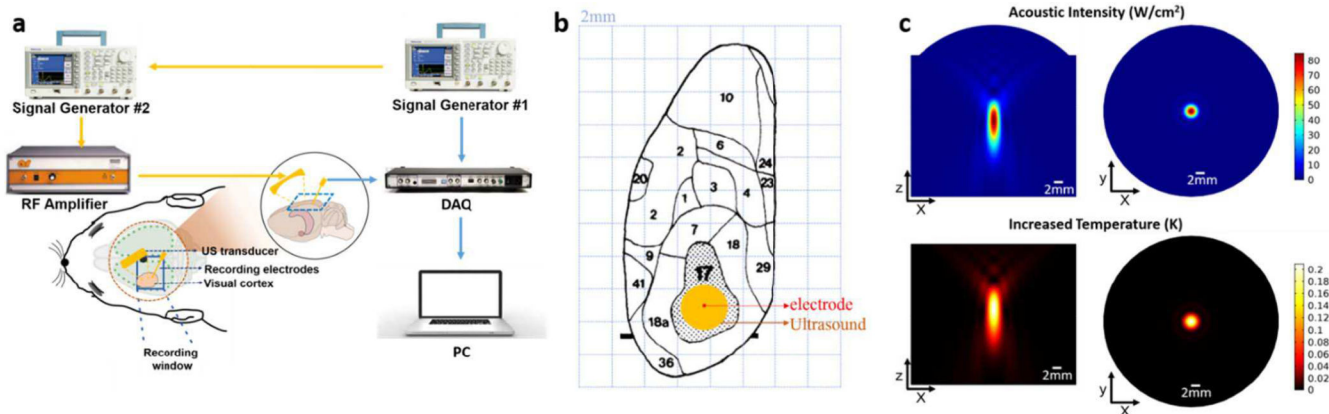


Fig. 1. (a) Schematic diagram of the experimental system. (b) The surface topography of the cortical areas of the left hemisphere of the rat, which was modified after Gabbott [28]. Each background grid has a length of 2mm. The primary visual cortex, area 17, is shown stippled. The exact position of the stereotaxically located electrode is shown by the red point. Ultrasound focal area is shown by the orange circle. (c) Top: Simulation results of spatial distribution of acoustic intensity. Bottom: Simulation results of the ultrasound-induced temperature increasing and its spatial distribution.

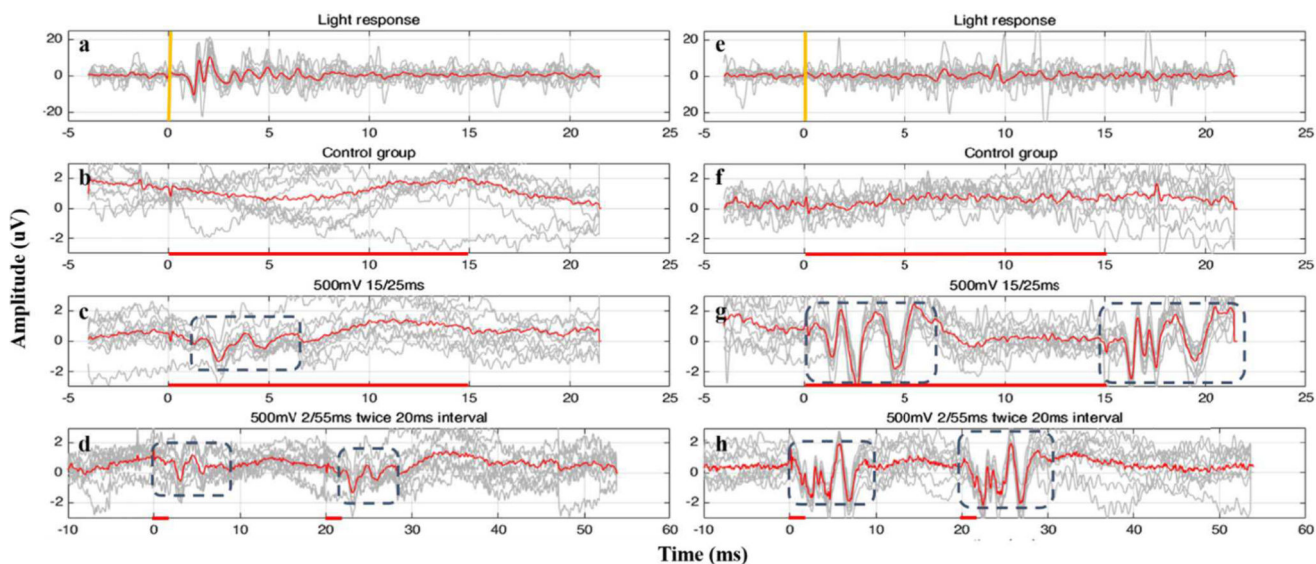


Fig. 2. Representative results evoked by continuous ultrasound stimulation from one normal rat (a-d) and one blind rat (e-h). Gray lines show eight-times records and red lines are the averaged records. Light stimulation was used to test the rats' visual responsiveness. Normal rats responded to the light (a) while blind rats failed to show any light responses (e). VC potential baseline recorded from during control experiments (when transducer was focused to a different direction) showed no responses in both rat groups (b)&(f). (c)&(g) show the responses with 15ms ultrasound stimulation (shown by the red line) from the group 1. (d)&(h) show the responses from the group 2.

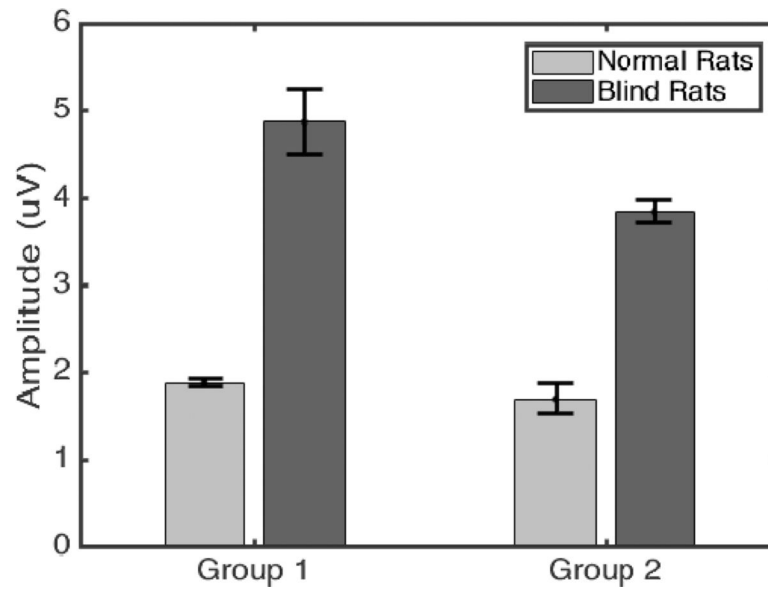


Fig. 3. Comparison of response amplitude in groups 1&2 showing blind rats have significantly stronger VC responses to US stimulation ($p < 0.001$, two-sample t-test). In experimental group 1, normal rats showed response amplitude of $1.88 \pm 0.04 \mu\text{V}$, whereas blind rats had $4.87 \pm 0.38 \mu\text{V}$. In group 2, the response amplitudes were $1.69 \pm 0.18 \mu\text{V}$ for normal rats and $3.84 \pm 0.14 \mu\text{V}$ for blind RCS rats.

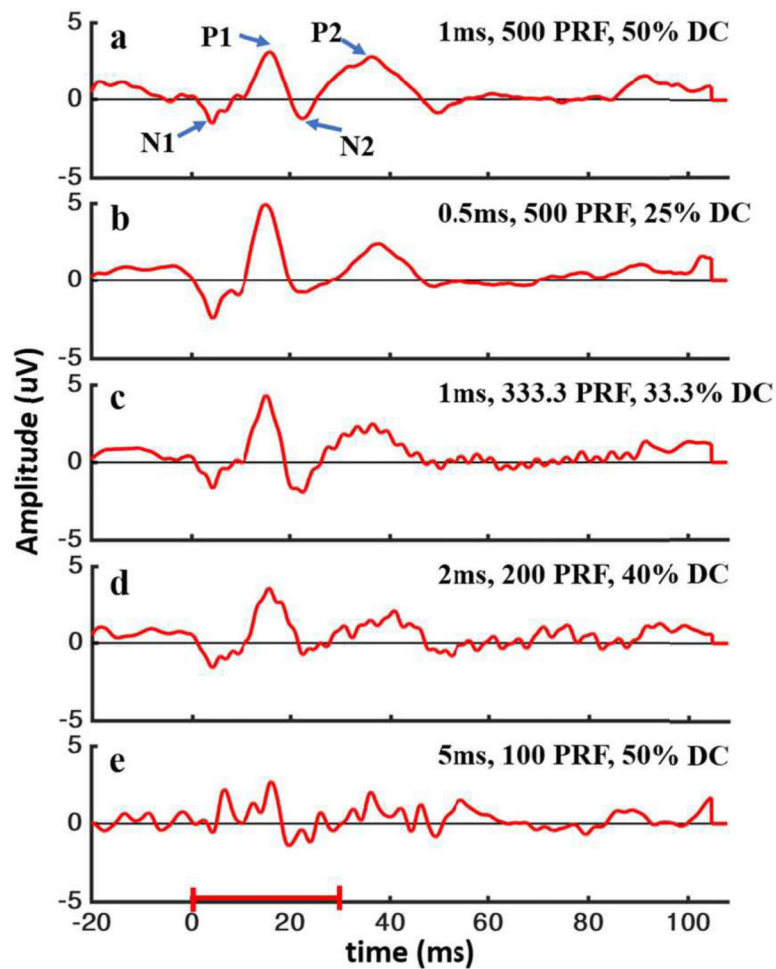


Fig. 4. VC low-frequency responses to pulsed US stimulation with high PRF. US stimulation duration was 30 ms, which shown by the red bar in the bottom. All signals were averaged 512 times. Signals were recorded with different stimulation parameters: (a) 1-ms pulse in every 2 ms (500PRF and 50% DC); (b) 0.5-ms pulse in every 2 ms (500PRF and 25% DC); (c) 1-ms pulse in every 3 ms (333.3PRF and 33.3% DC); (d) 2-ms pulse in every 5 ms (200PRF and 40% DC); (e) 5-ms pulse in every 10 ms (100PRF and 50% DC). Most responses (a)-(d) had a similar waveform which was labeled by P1, P2, N1, N2 in (a).